ISSN (Print) 1226-1750
ISSN (Online) 2233-6656
Journal of Magnetics 25(3), 330-334 (2020) https://doi.org/10.4283/JMAG.2020.25.3.330

Mn Doped CuO Nanoparticles Synthesized by Spray Pyrolysis: Structural, Optical and Magnetic Characterization

Ch. Hemalatha, K. Suresh Babu, and G. Narsinga Rao*

Department of Freshmen Engineering, Marri Laxman Reddy Institute of Technology and Management, Dundigal, Hyderabad 500 043, Telangana, India

(Received 3 May 2020, Received in final form 3 August 2020, Accepted 4 August 2020)

Pure and Mn (2.5 %, 5 % and 10 %) doped CuO nanoparticles were synthesized via chemical process of ultrasonic spray pyrolysis method. The crystal structure and grain size of the particles were determined using XRD. The optical properties of the samples were investigated using UV-Visible spectroscopy. The SEM micrographs revealed the surface morphology of sphere-shaped particles in all samples. The ZFC magnetization exhibits a sharp peak at 32 K and the FC magnetization saturated below this peak temperature. This is a characteristic feature of typical spin-glass behavior. In addition, the AC conductivity curves show an increasing conductivity value with increasing Mn content. The enhanced conductivity is due to the Mn doping in CuO induce defects in grain boundary.

Keywords : Copper oxide nanoparticles, ultrasonic spray pyrolysis method, Optical properties, spin-glass behavior

1. Introduction

Nanomaterials are not only a kind of ideal system for the study of many physical properties, but also possess potential applications in fabrication of electronic and optical nano-devices. Metal oxides span a broad range of properties from wide band-gap insulators to metallic and superconducting which creates a significant interest in the synthesis of metal oxide nanomaterials. Intensive research efforts have been devoted to the synthesis and investigation of the physical and chemical properties of semiconducting oxides

Metal oxides in particular span a significant interest in the synthesis of nanomaterials due to their specific physical properties and wide range of applications [1]. Semiconductor nanoparticles have unique optical and electrical properties when compared to that of bulk materials. Among all monoxides, Copper (II) oxide nanoparticles (CuO) belong to monoclinic structure system has wide range of potential applications due to enhanced physical and chemical properties [2-12]. They also possess a large surface to volume ratio [13].

Cupric oxide (CuO) is one of an important semiconducting oxide with a monoclinic structure and direct band gap of 1.85 eV [14, 15]. Copper oxide is a significant p-type nanomaterial and the properties of nanomaterials can be altered by changing the shape or morphology. Furthermore, the doping of the semiconductor with other ions can be done to enhance the physical and chemical properties of the materials [16-19]. Many authors have reported the improvement in material's characteristic properties using various dopants. It still remains a challenge to achieve pure and high quality of crystalline nanostructures. Among all, manganese, Mn, doping is known as an excellent catalyst of copper oxide [20, 21]. A number of methods are being proposed to fabricate nanomaterials of desired size and properties. The scope of the present work is to synthesize pure and Mn doped CuO nanoparticles with high quality and purity by chemical technique of ultrasonic spray pyrolysis. The structural, optical, morphological and compositional properties of the pure as well as Mn doped CuO nanoparticles have been investigated by X-ray Diffraction (XRD) analysis, UV–Visible Spectrophotometry, Scanning Electron Microscopy (SEM), Energy Dispersive Analysis of X-ray, magnetization and ac conductivity.

2. Experimental Procedure

The Copper (II) nitrate dihydrate ($Cu(NO_3)_2 \cdot 2H_2O$),

*Corresponding author: Tel: +91-8008092417
e-mail: nsrao.phys@gmail.com

Manganese nitrate tetrahydrate ($Mn(NO_3)_2{\cdot}4H_2O$) were used as precursor materials for the preparation of pure and Mn (2.5 %, 5 % and 10 %) doped CuO nanoparticles by ultrasonic spray pyrolysis. The raw materials used in the synthesis were analytical grade reagents from Merck company and used without further purification. During the synthesis of copper oxide nanoparticles, weighed amount of copper (II) nitrate dihydrate ($Cu(NO_3)_2{\cdot}2H_2O$) were dissolved in double distilled water to achieve 0.01 mole/L. The apparatus consists of an aerosol generator, an electrical heated reaction furnace carrying a quartz tube (670 mm length and 20 mm diameter) and a powder collection chamber. Only one transducer was implemented to create the aerosol. For this ultrasonic atomizing system, the resonant frequency was selected to 0.7 MHz. The experiments were carried out in the temperature range between 650 °C and 700 °C in air atmosphere with a flow rate of 0.5 L/min. For the Mn doped CuO samples, the same procedure was adopted with the addition of different concentrations (2.5 %, 5 % and 10 %) of $Mn(NO_3)_2{\cdot}4H_2O$ to Copper nitrate solution.

The crystal of the synthesized nanoparticles were studied by powder X-ray diffraction method (XRD) using a Philips PW-1710 x-ray diffractometer with CuKα radiation (λ = 1.54056 Å) in the 2θ range of 10-80° at room temperature. The absorption and transmittance properties of the samples were studied by ultraviolet-visible (UV-Vis) spectrometer in the visible wavelength range at room temperature. The morphology of the samples was obtained using Scanning electron microscope (Jeol JSM 6390) with energy dispersive analysis of x-ray (EDAX) at an accelerating voltage of 200 kV. The zero field cooled (ZFC) condition means the sample is cooled to 4 K without magnetic field and measured magnetic moment while heating the sample with applied magnetic field of 100 Oe. In field cooled (FC) condition the sample is cooled to 4 K with 100 Oe magnetic field and magnetic moment measured while heating the sample keep 100 Oe magnetic field. Both these magnetization curves were measured in a commercial SQUID magnetometer between 4 and 300 K in an applied field of 100 Oe.

3. Results and Discussion

The X-ray diffraction patterns (XRD) of CuO, $Cu_{0.975}Mn_{0.025}O$, $Cu_{0.95}Mn_{0.05}O$ and $Cu_{0.9}Mn_{0.1}O$ nanoparticles are shown in Fig. 1. In the diffraction pattern, all peaks are well indexed to the monoclinic phase of CuO with space group C2/c that was confirmed from JCPDS card No. 05-0661. The characteristic peaks located at 2θ = 31.7º, 35.5º, 38.6º, 45.4º, 53.4º, 57.9º, 61.4º, 66.2º, and 67.7º are assigned to (-110), (002), (111), (-112), (-202), (020), (202), (-113), (-310), and (220) plane orientation of CuO (JCPDS 05-0661). The main peaks at 2θ = 35.5º and 38.6º of nearly equal intensities corresponding to (002) and (111) planes are the characteristics peaks for monoclinic phase of pure CuO nanoparticles [14, 15]. Further no other impurity peak was observed in the XRD pattern showing the single phase sample formation of CuO nanoparticles. The Mn doped CuO is well crystalline and the predominant diffraction lines are same as that of undoped CuO. The crystallite size (d) was calculated using Debye-Scherrer's formula

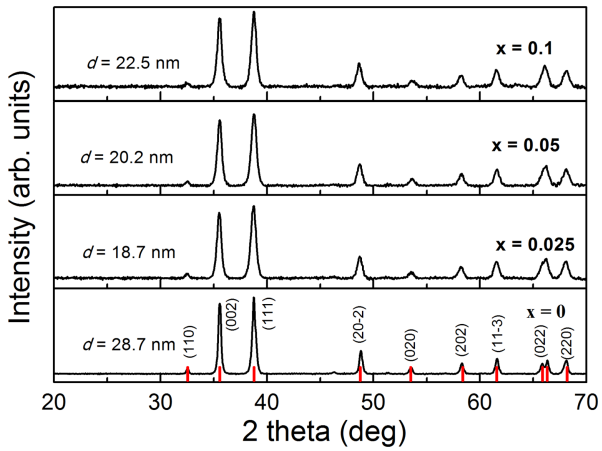

Fig. 1. (Color online) XRD patterns of $Cu_{1-x}Mn_xO$ nanoparticles with different doping concentration (x = 0, 0.025, 0.05, 0.10) and monoclinic structure Bragg peaks are marked as red marks.

$$d = 0.9\,\lambda/\beta\cos\theta$$

Where β is the full width at half maximum (FWHM) of the peak in XRD pattern, θ is angle of diffraction, λ is the wavelength of x-ray used which is 1.541 Å. The crystallite sizes are calculated using (002) and (111) peaks since the intensity of these two peaks is almost equal and the sizes for all samples are about 28.7, 18.7, 20.2 and 22.5 nm, corresponding to the CuO, $Cu_{0.975}Mn_{0.025}O$, $Cu_{0.95}Mn_{0.05}O$ and $Cu_{0.9}Mn_{0.1}O$, respectively.

The optical absorption properties of the synthesized CuO, $Cu_{0.975}Mn_{0.025}O$, $Cu_{0.95}Mn_{0.05}O$ and $Cu_{0.9}Mn_{0.1}O$ nanoparticles were analyzed by using UV–Visible spectrophotometer. The typical UV–Visible absorption spectra of the $Cu_{0.9}Mn_{0.1}O$ is displayed in Fig. 2. From this the band gap and the type of electronic transitions were determined. All the samples exhibit broad absorption peaks extending from UV to visible range. It has been observed that all the samples exhibit an absorption peak at around 291 nm, which is smaller than absorbance for bulk CuO which occurs at 310 nm as reported by Zhong *et al.* [4].

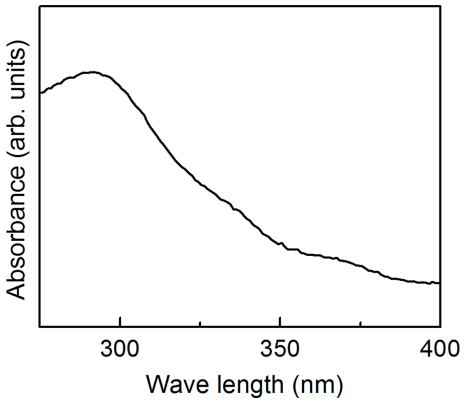

Fig. 2. Typical absorption spectra of $Cu_{1-x}Mn_xO$ nanoparticles as a function wavelength.

This shift towards lower wavelength could be attributed to the quantum confinement effect of nanoparticles. Optical band gap can be calculated from absorption spectrum using well known Tauc relation given by:

$$\alpha h\nu = A'(h\nu - Eg)^2$$

where α = 2.303 A/t is called the absorption coefficient, A is the absorbance, t is the path length of wave which is equal to the thickness of the cuvette, A' is the proportionality constant, Eg is the band gap, $h\nu$ is the photon energy and n = 1/2 and 2 for direct and indirect band gap semiconductors respectively. The band gap of all the nanoparticles are found to be around 2.6 eV which is larger than that of bulk CuO (1.85 eV). This increase has been attributed to the quantum confinement effect of nanoparticles. Further, the optical transmittance spectra

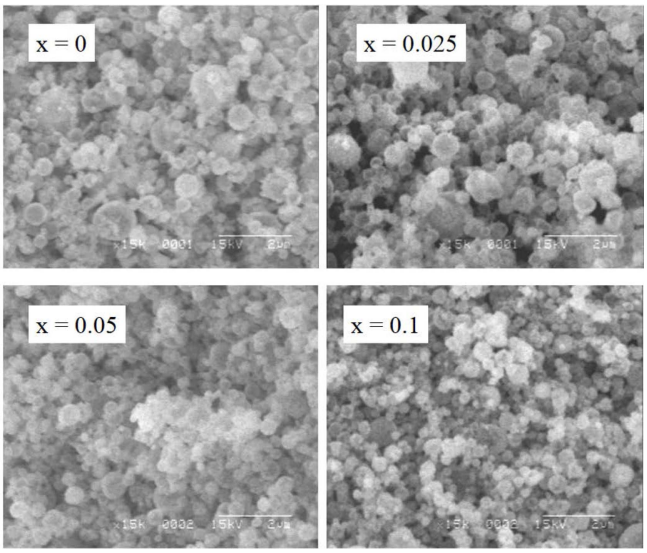

Fig. 3. SEM images of $Cu_{1-x}Mn_xO$ nanoparticles.

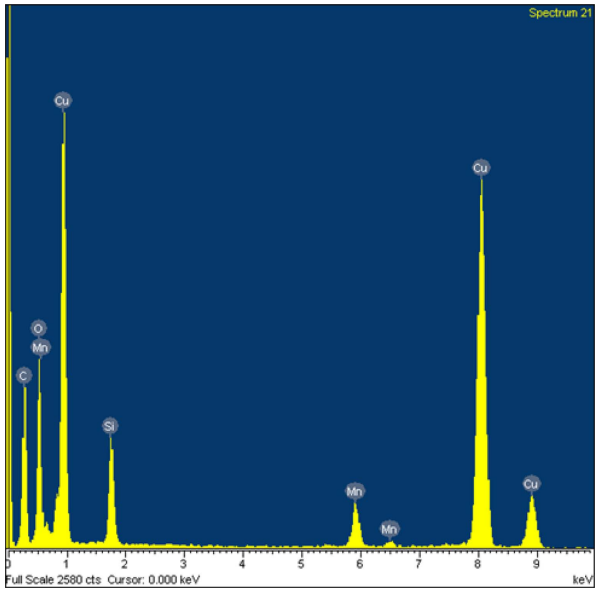

Fig. 4. (Color online) Typical EDAX spectra of $Cu_{0.95}Mn_{0.15}O$ particles.

show that Mn dopant increases the transmittance upto 88 %.

The morphology of the synthesized samples analyzed by SEM is shown in Fig. 3. SEM micrographs clearly exhibit almost spherical morphology of all the samples. Average crystallite size of undoped CuO nanoparticles are bigger than Mn doped nanoparticles. Moreover, with increasing Mn concentration crystallite size increases very small. The variation in particle size matches well with the XRD results. The presence of Mn in doped samples is confirmed from the selective area EDAX analysis. EDAX spectra of undoped CuO and 5 % Mn doped CuO nanoparticles are shown in Fig. 4. Since Mn is successfully incorporated in the system, it can be concluded that Mn is successfully doped in the CuO nanocrystals.

The typical temperature dependence of dc magnetization data were obtained in field cooled (FC) and zero field cooled (ZFC) cycles under an applied field of 100 Oe as shown in Fig. 5(a) for $Cu_{0.9}Mn_{0.1}O$ particles. Field cooled (FC) and zero field cooled (ZFC) susceptibility curves overlap at high temperature down to 20 K for x = 0.10 sample. The ZFC curve exhibits a sharp peak at 20 K and the FC curve saturated below this peak temperature. This is a characteristic feature of typical spin-glass behavior. Similar behavior were also observed for 5 and 2.5 % samples. With decreasing Mn content, the magnetic order is degraded due to more homogeneous host. Thus, in result the reduction of magnetization and the decrease of spin glass transition temperature were observed. The temperature dependence of the inverse magnetic suscepti-

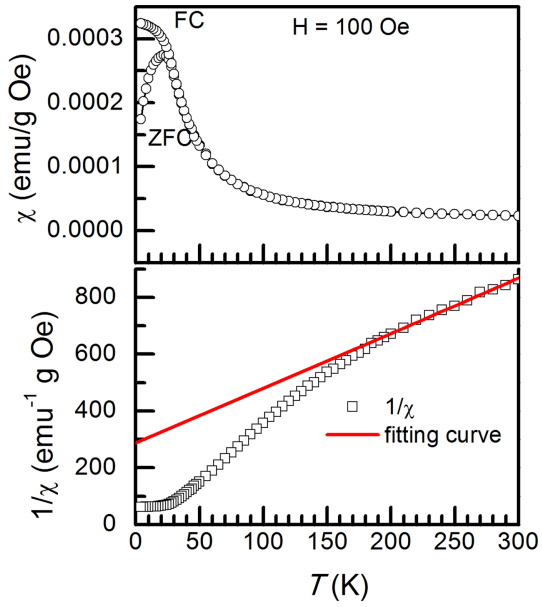

Fig. 5. (Color online) (a) c vs T curves of $Cu_{0.9}Mn_{0.1}O$ particles measured under a magnetic field of 100 Oe. (b) Inverse susceptibility vs T curve, solid red line indicates Curie Weiss law fitting.

bility ($1/\chi$) is also illustrated in Fig. 5(b). The solid line shows the Curie-Weiss law fitting $\chi = C/(T-\theta)$, where C and θ are the Curie constant and Curie-Weiss temperature, respectively. The calculated effective magnetic moment (μ_{eff}) is significantly larger than the theoretical value. This is attributed to an insufficient approximation of the Curie-Weiss formula. The large negative value of the Curie-Weiss temperature ($\theta = -150$ K) confirms the strong antiferromagnetic exchange coupling in these nanoparticles.

The ac conductivity (σ_{ac}) is calculated using the relation,

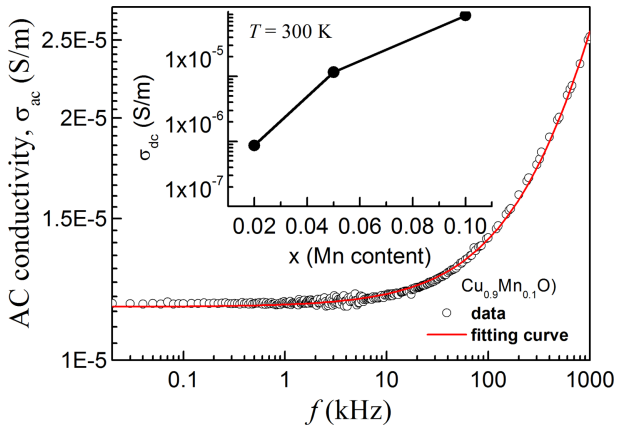

Fig. 6. (Color online) Typical Ac conductivity of $Cu_{0.9}Mn_{0.1}O$ nanoparticles as a function of frequency, solid red line indicates power law fitting. Inset depicts dc part of conductivity with x, Mn content.

$\sigma_{ac} = \omega\varepsilon'\varepsilon_0 \tan\delta$, where the symbols have their usual meanings.

The typical frequency-dependent conductivity curve at room temperature for $Cu_{0.9}Mn_{0.1}O$ nanoparticles are shown in Fig. 6. The ac conductivity is frequency independent at lower frequencies which are due to the dc part of conductivity. In conductivity spectra, the symbols represent the experimental data while solid lines represent the fitted results. Further, the ac conductivity is seemed to follow the Jonscher's power law [23]

$$\sigma_{ac} = \sigma_{dc} + A f^n$$

where σ_{dc} is the dc conductivity, 'A' determines the strength of polarizability, 'n' is the temperature dependent parameter whose value lies between 0.1 and 1 and it represents the degree of interaction between the mobile ions including the lattice and its vibrations with frequency and temperature. The AC conductivity is increase with increasing Mn content. The enhanced dc part of conductivity is shown in inset of Fig. 6. The synthesis processes of Mn doped CuO nanostructures and annihilation treatments are induce defects in grain boundary, because present all the samples are single phase without any impurity. These defects are mostly responsible for enhanced electrical conduction process of free charge carrier and formation of inhomogeneous dielectric structures in present samples, because the effect of morphology (all show spherical type) is negligible.

4. Conclusion

Pure and manganese doped copper oxide nanoparticles were synthesized via chemical process of ultrasonic spray pyrolysis method. XRD results show the formation of monoclinic structure and the average crystallite size was 18 to 28 nm. The band gap of all the nanoparticles are found to be around 2.6 eV which is larger than that of bulk CuO (1.85 eV). This increase has been attributed to the quantum confinement effect of nanoparticles. The enhanced transmittance of the synthesized nanoparticles from ultraviolet to the red region suggests that these particles could be employed as a host material for optoelectronic applications. SEM micrographs revealed that Mn is doped in CuO without disturbing the basic monoclinic structure. EDAX analysis also confirmed the presence of Mn dopant in the samples. The ZFC magnetization exhibits a sharp peak at 20 K and the FC magnetization saturated below this peak temperature. This is a characteristic feature of typical spin-glass behavior. In addition, the AC conductivity curves show an increasing conductivity value with increasing Mn content. The en-

hanced conductivity is due to the Mn doping in CuO induce defects in grain boundary.

Acknowledgements

This work is partially supported by the Department of Science and Technology (DST) No: SR/WOS-A/PM-39/2017 and Science & Engineering Research Board (SERB), Government of India, New Delhi, No: ECR/2016/001647.

References

[1] J. G. Hu, T. W. Odom, and C. M. Lieber, Accounts. Chem. Res **32**, 435 (1999).
[2] V. Ravishankar Rai and A. Jamuna Bai, In: Méndez-Vilas, A., Ed., Formatex, Microbiology Series, No. 3, Vol. 1, Spain, 197 (2011).
[3] S. C. Ray, Sol. Energy Mater. Sol. Cells **68**, 307 (2001).
[4] Z. Zhong, V. Ng, J. Luo, S. P. Teh, J. Teo, and A. Gedanken, Langmuir **23**, 5971 (2007).
[5] M. Arumugam, N. Santhamani, P. S. Kumar, and A. Sambandam, Sci. Adv. Mater. **2**, 51 (2010).
[6] Ji-Sang Hong, Journal of Magnetics **11**, 20 (2006).
[7] M. Frietsch, F. Zudock, J. Goschnick, and M. Bruns, Sensors Actuators B **65**, 379 (2000).
[8] P. Poizot, S. Laruelle, S. Grugeon, L. Dupont, and J. M. Taracon, Nature **407**, 496 (2000).
[9] D. P. Singh and N. Ali, Sci. Adv. Mater. **2**, 295 (2010).
[10] C. B. McAuley, Y. Du, G. G. Wildgoose, and R. G. Compton, Sensors Actuators B **135**, 230 (2008).
[11] L. Xu and J. J. Zhu, Sci. Adv. Mater. **1**, 121 (2009).
[12] A. Umar, M. M. Rahman, A. Al-Hajry, and Y. B. Hahn, Electrochem. Commun. **11**, 118 (2009).
[13] A. Henglein, Chem. Rev. **89**, 1861 (1989).
[14] K. Sanfra, C. K. Sarkar, M. K. Mukherjee, and B. Ghosh, Thin Solid Films **213**, 226 (1992).
[15] D. M. Fernandes, R. Silva, A. A. W. Hechenleitner, E. Radovanovic, M. A. C. Melo, and E. A. G. Pineda, Mater. Chem. Phys. **115**, 110 (2009).
[16] M. Chang, H. Liu, and C. Y. Tai, Powder Technology **207**, 378 (2011).
[17] H. Wang, J. Xu, J. Zhu, and H. Chen, J. Cryst. Growth **244**, 88 (2002).
[18] A. S. Ahmed, S. M. Muhamed, M. L. Singla, S. Tabassum, A. H. Naqvi, and A. Azam, J. Lumin. **131**, 1 (2011).
[19] K. Das, S. N. Sharma, M. Kumar, and S. K. De, J. Appl. Phys. **107**, 024316 (2010).
[20] Hongyan Cao, Xiaoshuang Li, Yaoqiang Chen, Maochu Gong, and Jianli Wang, J. Rare Earths **30**, 871 (2012).
[21] J. M. Wesselinowa, Physics Letters A **375**, 1417 (2011).
[22] J. A. Mydosh, Spin Glasses: An Experimental Introduction (Taylor & Francis, London, Washington DC, 1996).
[23] A. K. Jonscher, Nature **267**, 673 (1977).